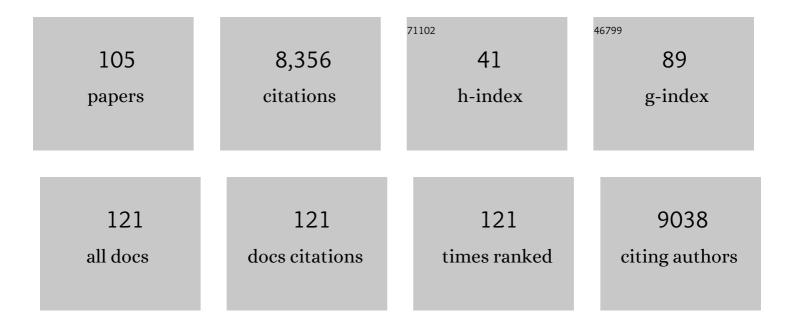
David E Graham

List of Publications by Year in descending order

Source: https://exaly.com/author-pdf/1901479/publications.pdf Version: 2024-02-01



ΠΛΛΙΠ Ε ΩΡΛΗΛΜ

#	Article	IF	CITATIONS
1	Unravelling biogeochemical drivers of methylmercury production in an Arctic fen soil and a bog soil. Environmental Pollution, 2022, 299, 118878.	7.5	8
2	Quantifying pH buffering capacity in acidic, organic-rich Arctic soils: Measurable proxies and implications for soil carbon degradation. Geoderma, 2022, 424, 116003.	5.1	7
3	Anaerobic respiration pathways and response to increased substrate availability of Arctic wetland soils. Environmental Sciences: Processes and Impacts, 2020, 22, 2070-2083.	3.5	6
4	Influences of Hillslope Biogeochemistry on Anaerobic Soil Organic Matter Decomposition in a Tundra Watershed. Journal of Geophysical Research G: Biogeosciences, 2020, 125, e2019JG005512.	3.0	4
5	Temporal, Spatial, and Temperature Controls on Organic Carbon Mineralization and Methanogenesis in Arctic High-Centered Polygon Soils. Frontiers in Microbiology, 2020, 11, 616518.	3.5	3
6	Temperature sensitivity of mineral-enzyme interactions on the hydrolysis of cellobiose and indican by β-glucosidase. Science of the Total Environment, 2019, 686, 1194-1201.	8.0	20
7	Expression of benzoyl-CoA metabolism genes in the lignocellulolytic host Caldicellulosiruptor bescii. AMB Express, 2019, 9, 59.	3.0	1
8	Soil Aggregate Microbial Communities: Towards Understanding Microbiome Interactions at Biologically Relevant Scales. Applied and Environmental Microbiology, 2019, 85, .	3.1	233
9	Modeling anaerobic soil organic carbon decomposition in Arctic polygon tundra: insights into soil geochemical influences on carbon mineralization. Biogeosciences, 2019, 16, 663-680.	3.3	21
10	Stimulation of anaerobic organic matter decomposition by subsurface organic N addition in tundra soils. Soil Biology and Biochemistry, 2019, 130, 195-204.	8.8	13
11	Cryomilled zinc sulfide: A prophylactic for <i>Staphylococcus aureus</i> -infected wounds. Journal of Biomaterials Applications, 2018, 33, 82-93.	2.4	0
12	Characterization of iron oxide nanoparticle films at the air–water interface in Arctic tundra waters. Science of the Total Environment, 2018, 633, 1460-1468.	8.0	8
13	Impacts of Methane on Carbon Dioxide Storage in Brine Formations. Ground Water, 2018, 56, 176-186.	1.3	35
14	Influence of Structural Defects on Biomineralized ZnS Nanoparticle Dissolution: An in-Situ Electron Microscopy Study. Environmental Science & Technology, 2018, 52, 1139-1149.	10.0	42
15	Molecular Insights into Arctic Soil Organic Matter Degradation under Warming. Environmental Science & Technology, 2018, 52, 4555-4564.	10.0	74
16	Impacts of temperature and soil characteristics on methane production and oxidation in Arctic tundra. Biogeosciences, 2018, 15, 6621-6635.	3.3	33
17	Improved ZnS nanoparticle properties through sequential NanoFermentation. Applied Microbiology and Biotechnology, 2018, 102, 8329-8339.	3.6	2
18	Transport of perfluorocarbon tracers in the Cranfield Geological Carbon Sequestration Project. , 2018, 8, 650-671.		11

#	Article	IF	CITATIONS
19	Iron-Dependent Enzyme Catalyzes the Initial Step in Biodegradation of <i>N</i> -Nitroglycine by Variovorax sp. Strain JS1663. Applied and Environmental Microbiology, 2017, 83, .	3.1	11
20	Influence of iron redox cycling on organo-mineral associations in Arctic tundra soil. Geochimica Et Cosmochimica Acta, 2017, 207, 210-231.	3.9	94
21	UV-activated ZnO films on a flexible substrate for room temperature O2 and H2O sensing. Scientific Reports, 2017, 7, 6053.	3.3	61
22	Mathematical Modelling of Arctic Polygonal Tundra with <i>Ecosys</i> : 1. Microtopography Determines How Active Layer Depths Respond to Changes in Temperature and Precipitation. Journal of Geophysical Research G: Biogeosciences, 2017, 122, 3161-3173.	3.0	38
23	Microbial Community and Functional Gene Changes in Arctic Tundra Soils in a Microcosm Warming Experiment. Frontiers in Microbiology, 2017, 8, 1741.	3.5	26
24	Biogeochemical modeling of CO ₂ and CH ₄ production in anoxic Arctic soil microcosms. Biogeosciences, 2016, 13, 5021-5041.	3.3	27
25	Reviews and syntheses: Four decades of modeling methane cycling in terrestrial ecosystems. Biogeosciences, 2016, 13, 3735-3755.	3.3	102
26	Multi-spectral Infrared Computed Tomography. IS&T International Symposium on Electronic Imaging, 2016, 28, 1-5.	0.4	1
27	Draft Genome Sequence of Streptomyces vitaminophilus ATCC 31673, a Producer of Pyrrolomycin Antibiotics, Some of Which Contain a Nitro Group. Genome Announcements, 2016, 4, .	0.8	1
28	Manufacturing demonstration of microbially mediated zinc sulfide nanoparticles in pilot-plant scale reactors. Applied Microbiology and Biotechnology, 2016, 100, 7921-7931.	3.6	32
29	Simulating the Cranfield geological carbon sequestration project with high-resolution static models and an accurate equation of state. International Journal of Greenhouse Gas Control, 2016, 54, 282-296.	4.6	72
30	Warming increases methylmercury production in an Arctic soil. Environmental Pollution, 2016, 214, 504-509.	7.5	60
31	Potential carbon emissions dominated by carbon dioxide from thawed permafrost soils. Nature Climate Change, 2016, 6, 950-953.	18.8	288
32	Active layer hydrology in an arctic tundra ecosystem: quantifying water sources and cycling using water stable isotopes. Hydrological Processes, 2016, 30, 4972-4986.	2.6	68
33	Effects of warming on the degradation and production of low-molecular-weight labile organic carbon in an Arctic tundra soil. Soil Biology and Biochemistry, 2016, 95, 202-211.	8.8	57
34	Surface reflectance degradation by microbial communities. Journal of Building Physics, 2016, 40, 263-277.	2.4	3
35	Pathways of anaerobic organic matter decomposition in tundra soils from Barrow, Alaska. Journal of Geophysical Research G: Biogeosciences, 2015, 120, 2345-2359.	3.0	41
36	A microbial functional groupâ€based module for simulating methane production and consumption: Application to an incubated permafrost soil. Journal of Geophysical Research G: Biogeosciences, 2015, 120, 1315-1333.	3.0	56

#	Article	IF	CITATIONS
37	Geochemical drivers of organic matter decomposition in arctic tundra soils. Biogeochemistry, 2015, 126, 397-414.	3.5	53
38	Microtopographic and depth controls on active layer chemistry in Arctic polygonal ground. Geophysical Research Letters, 2015, 42, 1808-1817.	4.0	44
39	lsotopic identification of soil and permafrost nitrate sources in an Arctic tundra ecosystem. Journal of Geophysical Research G: Biogeosciences, 2015, 120, 1000-1017.	3.0	22
40	Stoichiometry and temperature sensitivity of methanogenesis and <scp>CO</scp> ₂ production from saturated polygonal tundra in Barrow, Alaska. Global Change Biology, 2015, 21, 722-737.	9.5	68
41	Size tunable elemental copper nanoparticles: extracellular synthesis by thermoanaerobic bacteria and capping molecules. Journal of Materials Chemistry C, 2015, 3, 644-650.	5.5	39
42	<i>In situ</i> capping for size control of monochalcogenide (ZnS, CdS and SnS) nanocrystals produced by anaerobic metal-reducing bacteria. Nanotechnology, 2015, 26, 325602.	2.6	13
43	Direct determination of protonation states and visualization of hydrogen bonding in a glycoside hydrolase with neutron crystallography. Proceedings of the National Academy of Sciences of the United States of America, 2015, 112, 12384-12389.	7.1	35
44	Indexing Permafrost Soil Organic Matter Degradation Using High-Resolution Mass Spectrometry. PLoS ONE, 2015, 10, e0130557.	2.5	78
45	L-Arabinose Binding, Isomerization, and Epimerization by D-Xylose Isomerase: X-Ray/Neutron Crystallographic and Molecular Simulation Study. Structure, 2014, 22, 1287-1300.	3.3	22
46	Engineering acidic Streptomyces rubiginosus D-xylose isomerase by rational enzyme design. Protein Engineering, Design and Selection, 2014, 27, 59-64.	2.1	19
47	Improvement of cellulose catabolism in Clostridium cellulolyticum by sporulation abolishment and carbon alleviation. Biotechnology for Biofuels, 2014, 7, 25.	6.2	25
48	X-ray crystallographic studies of family 11 xylanase Michaelis and product complexes: implications for the catalytic mechanism. Acta Crystallographica Section D: Biological Crystallography, 2014, 70, 11-23.	2.5	34
49	Insights into archaeal evolution and symbiosis from the genomes of a nanoarchaeon and its inferred crenarchaeal host from Obsidian Pool, Yellowstone National Park. Biology Direct, 2013, 8, 9.	4.6	102
50	Nitrogen and sulfur requirements for Clostridium thermocellum and Caldicellulosiruptor bescii on cellulosic substrates in minimal nutrient media. Bioresource Technology, 2013, 130, 125-135.	9.6	33
51	Heterologous expression, purification, crystallization and preliminary X-ray analysis ofTrichoderma reeseixylanase II and four variants. Acta Crystallographica Section F: Structural Biology Communications, 2013, 69, 320-323.	0.7	2
52	Microbes in thawing permafrost: the unknown variable in the climate change equation. ISME Journal, 2012, 6, 709-712.	9.8	153
53	Combined inactivation of the Clostridium cellulolyticum lactate and malate dehydrogenase genes substantially increases ethanol yield from cellulose and switchgrass fermentations. Biotechnology for Biofuels, 2012, 5, 2.	6.2	125
54	Label-free Quantitative Proteomics for the Extremely Thermophilic Bacterium <i>Caldicellulosiruptor obsidiansis</i> Reveal Distinct Abundance Patterns upon Growth on Cellobiose, Crystalline Cellulose, and Switchgrass. Journal of Proteome Research, 2011, 10, 5302-5314.	3.7	33

#	Article	IF	CITATIONS
55	Use of Label-Free Quantitative Proteomics To Distinguish the Secreted Cellulolytic Systems of Caldicellulosiruptor bescii and Caldicellulosiruptor obsidiansis. Applied and Environmental Microbiology, 2011, 77, 4042-4054.	3.1	71
56	2-Oxoacid Metabolism in Methanogenic CoM and CoB Biosynthesis. Methods in Enzymology, 2011, 494, 301-326.	1.0	10
57	A new role for coenzyme F ₄₂₀ in aflatoxin reduction by soil mycobacteria. Molecular Microbiology, 2010, 78, 533-536.	2.5	9
58	Complete Genome Sequence of the Cellulolytic Thermophile <i>Caldicellulosiruptor obsidiansis</i> OB47 ^T . Journal of Bacteriology, 2010, 192, 6099-6100.	2.2	39
59	Substrate Specificity Determinants of the Methanogen Homoaconitase Enzyme: Structure and Function of the Small Subunit [,] . Biochemistry, 2010, 49, 2687-2696.	2.5	18
60	Archaeal ApbC/Nbp35 Homologs Function as Iron-Sulfur Cluster Carrier Proteins. Journal of Bacteriology, 2009, 191, 1490-1497.	2.2	52
61	Transcriptional Regulation of the <i>Escherichia coli</i> Gene <i>rraB</i> , Encoding a Protein Inhibitor of RNase E. Journal of Bacteriology, 2009, 191, 6665-6674.	2.2	12
62	Independent inactivation of arginine decarboxylase genes by nonsense and missense mutations led to pseudogene formation in Chlamydia trachomatisserovar L2 and D strains. BMC Evolutionary Biology, 2009, 9, 166.	3.2	13
63	Convergent evolution of coenzyme M biosynthesis in the Methanosarcinales: cysteate synthase evolved from an ancestral threonine synthase. Biochemical Journal, 2009, 424, 467-478.	3.7	43
64	Enzymatic analysis of uridine diphosphate N-acetyl-d -glucosamine. Analytical Biochemistry, 2008, 381, 94-100.	2.4	27
65	Methanogens with pseudomurein use diaminopimelate aminotransferase in lysine biosynthesis. FEBS Letters, 2008, 582, 1369-1374.	2.8	9
66	Crenarchaeal Arginine Decarboxylase Evolved from an S-Adenosylmethionine Decarboxylase Enzyme. Journal of Biological Chemistry, 2008, 283, 25829-25838.	3.4	42
67	Acetamido Sugar Biosynthesis in the Euryarchaea. Journal of Bacteriology, 2008, 190, 2987-2996.	2.2	46
68	A korarchaeal genome reveals insights into the evolution of the Archaea. Proceedings of the National Academy of Sciences of the United States of America, 2008, 105, 8102-8107.	7.1	253
69	Outer and Inner Membrane Proteins Compose an Arginine-Agmatine Exchange System in <i>Chlamydophila pneumoniae</i> . Journal of Bacteriology, 2008, 190, 7431-7440.	2.2	11
70	Methanogen Homoaconitase Catalyzes Both Hydrolyase Reactions in Coenzyme B Biosynthesis. Journal of Biological Chemistry, 2008, 283, 28888-28896.	3.4	31
71	Identification and Characterization of Archaeal and Fungal tRNA Methyltransferases. Methods in Enzymology, 2007, 425, 185-209.	1.0	1
72	Characterization of an Acid-Dependent Arginine Decarboxylase Enzyme from Chlamydophila pneumoniae. Journal of Bacteriology, 2007, 189, 7376-7383.	2.2	16

David E Graham

#	Article	IF	CITATIONS
73	Yeast Mitochondrial Initiator tRNA Is Methylated at Guanosine 37 by the Trm5-encoded tRNA (Guanine-N1-)-methyltransferase. Journal of Biological Chemistry, 2007, 282, 27744-27753.	3.4	52
74	Biosynthesis of Phosphoserine in the Methanococcales. Journal of Bacteriology, 2007, 189, 575-582.	2.2	43
75	Enzymology and Evolution of the Pyruvate Pathway to 2-Oxobutyrate in Methanocaldococcus jannaschii. Journal of Bacteriology, 2007, 189, 4391-4400.	2.2	55
76	Acetyl-coenzyme A Synthases and Nickel-Containing Carbon Monoxide Dehydrogenases. , 2007, , 357-415.		13
77	Identification and characterization of a -tyrosine decarboxylase in. Biochimica Et Biophysica Acta - General Subjects, 2005, 1722, 175-182.	2.4	36
78	Complete Genome Sequence of the Genetically Tractable Hydrogenotrophic Methanogen Methanococcus maripaludis. Journal of Bacteriology, 2004, 186, 6956-6969.	2.2	208
79	Identification of the 7,8-didemethyl-8-hydroxy-5-deazariboflavin synthase required for coenzyme F 420 biosynthesis. Archives of Microbiology, 2003, 180, 455-464.	2.2	66
80	Pyruvoyl-Dependent Arginine Decarboxylase from Methanococcus jannaschii. Structure, 2003, 11, 285-294.	3.3	34
81	Reductive dehalogenation of monobromobimane by tris(2-carboxyethyl)phosphine. Analytical Biochemistry, 2003, 318, 325-328.	2.4	11
82	The Methanococcus jannaschiidCTP Deaminase Is a Bifunctional Deaminase and Diphosphatase. Journal of Biological Chemistry, 2003, 278, 11100-11106.	3.4	26
83	Glutathione synthetase homologs encode Â-L-glutamate ligases for methanogenic coenzyme F420 and tetrahydrosarcinapterin biosyntheses. Proceedings of the National Academy of Sciences of the United States of America, 2003, 100, 9785-9790.	7.1	52
84	Phosphoprotein with Phosphoglycerate Mutase Activity from the Archaeon Sulfolobus solfataricus. Journal of Bacteriology, 2003, 185, 2112-2121.	2.2	24
85	The genome of Nanoarchaeum equitans: Insights into early archaeal evolution and derived parasitism. Proceedings of the National Academy of Sciences of the United States of America, 2003, 100, 12984-12988.	7.1	488
86	The Structural Determination of Phosphosulfolactate Synthase from Methanococcus jannaschii at 1.7-Ã Resolution. Journal of Biological Chemistry, 2003, 278, 45858-45863.	3.4	16
87	Transfer RNA-dependent amino acid biosynthesis: An essential route to asparagine formation. Proceedings of the National Academy of Sciences of the United States of America, 2002, 99, 2678-2683.	7.1	91
88	Identification of Coenzyme M Biosynthetic Phosphosulfolactate Synthase. Journal of Biological Chemistry, 2002, 277, 13421-13429.	3.4	79
89	Methanococcus jannaschii Uses a Pyruvoyl-dependent Arginine Decarboxylase in Polyamine Biosynthesis. Journal of Biological Chemistry, 2002, 277, 23500-23507.	3.4	46
90	Orthologs of a novel archaeal and of the bacterial peptidyl-tRNA hydrolase are nonessential in yeast. Proceedings of the National Academy of Sciences of the United States of America, 2002, 99, 16707-16712.	7.1	64

#	Article	IF	CITATIONS
91	The Genome of <i>M. acetivorans</i> Reveals Extensive Metabolic and Physiological Diversity. Genome Research, 2002, 12, 532-542.	5.5	573
92	Elucidation of methanogenic coenzyme biosyntheses: from spectroscopy to genomics. Natural Product Reports, 2002, 19, 133-147.	10.3	109
93	A Member of a New Class of GTP Cyclohydrolases Produces Formylaminopyrimidine Nucleotide Monophosphatesâ€. Biochemistry, 2002, 41, 15074-15084.	2.5	40
94	A divergent archaeal member of the alkaline phosphatase binuclear metalloenzyme superfamily has phosphoglycerate mutase activity. FEBS Letters, 2002, 517, 190-194.	2.8	27
95	Identification of coenzyme M biosynthetic 2-phosphosulfolactate phosphatase FEBS Journal, 2001, 268, 5176-5188.	0.2	32
96	Transfer Region of a Bacteroides Conjugative Transposon, CTnDOT. Plasmid, 2001, 45, 41-51.	1.4	39
97	Genome of Methanocaldococcus (methanococcus) jannaschii. Methods in Enzymology, 2001, 330, 40-123.	1.0	18
98	Post-transcriptional modification in archaeal tRNAs: identities and phylogenetic relations of nucleotides from mesophilic and hyperthermophilic Methanococcales. Nucleic Acids Research, 2001, 29, 4699-4706.	14.5	114
99	A dual-specificity aminoacyl-tRNA synthetase in the deep-rooted eukaryote Giardia lamblia. Proceedings of the National Academy of Sciences of the United States of America, 2000, 97, 12997-13002.	7.1	43
100	Identification of a Highly Diverged Class ofS-Adenosylmethionine Synthetases in the Archaea. Journal of Biological Chemistry, 2000, 275, 4055-4059.	3.4	47
101	S-Adenosylmethionine Decarboxylase from the Archaeon Methanococcus jannaschii: Identification of a Novel Family of Pyruvoyl Enzymes. Journal of Bacteriology, 2000, 182, 6667-6672.	2.2	25
102	An archaeal genomic signature. Proceedings of the National Academy of Sciences of the United States of America, 2000, 97, 3304-3308.	7.1	74
103	Cysteinyl-tRNA formation: the last puzzle of aminoacyl-tRNA synthesis. FEBS Letters, 1999, 462, 302-306.	2.8	27
104	The complete genome of the hyperthermophilic bacterium Aquifex aeolicus. Nature, 1998, 392, 353-358.	27.8	1,120
105	The complete genome sequence of the hyperthermophilic, sulphate-reducing archaeon Archaeoglobus fulgidus. Nature, 1997, 390, 364-370.	27.8	1,460